CIRCADIAN RHYTHMS

The hepatocyte clock and feeding control chronophysiology of multiple liver cell types

Dongyin Guan[1,2], Ying Xiong[1,2], Trang Minh Trinh[1,2], Yang Xiao[1,2], Wenxiang Hu[1,2], Chunjie Jiang[1,2], Pieterjan Dierickx[1,2], Cholsoon Jang[3]*, Joshua D. Rabinowitz[3], Mitchell A. Lazar[1,2,4]†

Most cells of the body contain molecular clocks, but the requirement of peripheral clocks for rhythmicity and their effects on physiology are not well understood. We show that deletion of core clock components REV-ERBα and REV-ERBβ in adult mouse hepatocytes disrupts diurnal rhythms of a subset of liver genes and alters the diurnal rhythm of de novo lipogenesis. Liver function is also influenced by nonhepatocytic cells, and the loss of hepatocyte REV-ERBs remodels the rhythmic transcriptomes and metabolomes of multiple cell types within the liver. Finally, alteration of food availability demonstrates the hierarchy of the cell-intrinsic hepatocyte clock mechanism and the feeding environment. Together, these studies reveal previously unsuspected roles of the hepatocyte clock in the physiological coordination of nutritional signals and cell-cell communication controlling rhythmic metabolism.

Biological rhythms are intricately involved in sleeping-waking, feeding-fasting, and activity-rest phenomena, and they are essential to maintaining physiological homeostasis (*1*). The mammalian core clock includes transcriptional activators BMAL1/CLOCK and transcriptional repressors REV-ERBα and REV-ERBβ that function in interlocked transcriptional feedback loops (*2*). Central clocks in the suprachiasmatic nucleus (SCN) are believed to synchronize clocks in peripheral tissues (*3*), and dyssynchrony of this system is associated with metabolic dysfunction (*4*, *5*). Nevertheless, major questions remain as to how the environment and genetic factors control the clocks in peripheral tissues and whether communication exists between clocks in different cell types within an organ.

To dissect the cell-autonomous and nonautonomous regulation of diurnal rhythms in peripheral tissues, we focused on the liver, a metabolic hub (*6*). REV-ERBα and REV-ERBβ were specifically deleted in hepatocytes (HepDKO; DKO, double knockout) by injecting the AAV8-TBG-CRE virus into adult REV-ERBα/β floxed mice. This model excludes developmental effects and potential confounding due to direct manipulation of the clock in other tissues (*7*, *8*). Expression of both REV-ERBα and REV-ERBβ was nearly undetectable after 2 weeks, even at zeitgeber time 10 (ZT10), when REV-ERBs were highly expressed at the mRNA (Fig. 1A) and protein level (fig. S1). REV-ERBs physiologically repress *Bmal1* and *Npas2* in a circadian manner (*9*, *10*), and both of these genes were constitutively derepressed in the REV-ERB HepDKO (Fig. 1B). Other core clock genes also demonstrated reduced rhythmicity (Fig. 1B).

We next examined the effect of REV-ERB HepDKO on the liver rhythmic transcriptome. Two weeks after adeno-associated virus (AAV) treatment, RNA sequencing (RNA-seq) performed on livers harvested every 3 hours revealed the attenuation of the rhythmicity of a large group of transcripts that were highly rhythmic in the controls, including genes involved in diurnal rhythm pathways such as *Bmal1*, *Npas2*, and *Clock* (Fig. 1C, fig. S2A, and table S1A). This observation fits the prevailing hypothesis that REV-ERBs are major controllers of the clock and suggests that the rhythmic expression of these genes depends on the intrinsic core clock feedback loop. Many genes, however, maintained diurnal rhythmicity in the absence of REV-ERBs (Fig. 1D, fig. S2B, and table S1B). Among these were ~170 genes, enriched for lipid metabolism, that showed enhanced rhythmic amplitudes (Fig. 1E, fig. S2C, and table S1C). KEGG (Kyoto Encyclopedia of Genes and Genomes) and gene set enrichment analysis (GSEA) indicated that rhythmic transcripts regulated by REV-ERBs were involved in circadian rhythms, hormone secretion, and lipid metabolism (fig. S2, A to D). These results indicated an unexpected rhythmic transcriptomic reprogramming in the liver upon the depletion of REV-ERBs in adult hepatocytes. Importantly, rhythmic locomotor activity (fig. S3A), feeding (fig. S3B), and plasma insulin levels (fig. S3C) were not much affected in REV-ERB HepDKO mice, indicating that disruption of the hepatocyte clock did not affect diurnal activity and feeding responses and excluding the possibility that the remodeling of the liver rhythmic transcriptome was due to changes in behavior.

Rhythmic expression of REV-ERB directly regulates many target genes by binding to ROR/REV-ERB-response element (RORE), where it represses transcription by recruiting co-repressors, by competing with ROR nuclear receptors, and by tethering to liver factors (*11*). ROR targets represented a high percentage of rhythm disrupted but not enhanced transcripts (fig. S3D), suggesting that REV-ERB's direct binding was more relevant to the rhythmically disrupted transcripts. Rhythmic transcriptome remodeling was confirmed in livers expressing REV-ERBα DNA binding domain deficient mutant and lacking REV-ERBβ (fig. S3E) (*12*).

To explore the transcriptional mechanism underlying rhythmic disruption in hepatocytes upon REV-ERB HepDKO, we used CistromeDB (*13*) to perform transcription factor (TF) binding similarity screening based on all published liver cistromes. REV-ERBs and their co-repressors HDAC3 and NCOR1 were the top TFs bound near genes whose diurnal rhythm was disrupted by REV-ERB HepDKO (Fig. 1F and table S2A). The binding sites of BMAL1, PER2, and CRY1 were enriched in rhythm-retained transcripts, suggesting that systemic signals drive rhythmic gene expression via these core clock genes (*14*) (fig. S3F and table S2B).

Although there is no REV-ERBα binding site near *Srebf1*, SREBF1 was the most enriched TF near genes whose diurnal rhythms were induced by the loss of REV-ERBs (Fig. 1G and table S2C). The rhythmic expression of *Srebf1* was enhanced upon REV-ERB HepDKO, as was that of many of its target genes that are involved in de novo lipogenesis (DNL) (Fig. 1H), which is consistent with a previous REV-ERBα whole-body knockout mouse model (*15*). Enhanced diurnal rhythmic expression of *Srebf1* was also observed in livers from reverse phase feeding (RPF) $Cry1^{-/-}$;$Cry2^{-/-}$ mice (*16*), suggesting a general role of core clock TF repressors in maintaining the homeostasis of hepatic lipid metabolism. The physiological significance of this finding was assessed by directly measuring DNL using deuterated water as a tracer. Consistent with the enhanced rhythm of *Srebf1* and the DNL pathway, the normal rhythm of DNL was markedly amplified in the livers of the REV-ERB HepDKO mice (Fig. 1I). This amplification was accompanied by an increase in the amplitude of plasma triglyceride rhythms, both on normal chow (Fig. 1J) and on high-fat, high-sucrose (HFHS) diet (Fig. 1K). Consistent with the increase in DNL, liver TG concentration was also increased in the livers of the HFHS-fed mice (Fig. 1L). Thus, REV-ERBs in hepatocytes

[1]Institute for Diabetes, Obesity, and Metabolism, Perelman School of Medicine, University of Pennsylvania, Philadelphia, PA 19104, USA. [2]Division of Endocrinology, Diabetes, and Metabolism, Department of Medicine, Perelman School of Medicine, University of Pennsylvania, Philadelphia, PA 19104, USA. [3]Lewis-Sigler Institute for Integrative Genomics and Department of Chemistry, Princeton University, Princeton, NJ 08544, USA. [4]Department of Genetics, Perelman School of Medicine, University of Pennsylvania, Philadelphia, PA 19104, USA.
*Present address: Department of Biological Chemistry, University of California Irvine, Irvine, CA 92697, USA.
†Corresponding author. Email: lazar@pennmedicine.upenn.edu

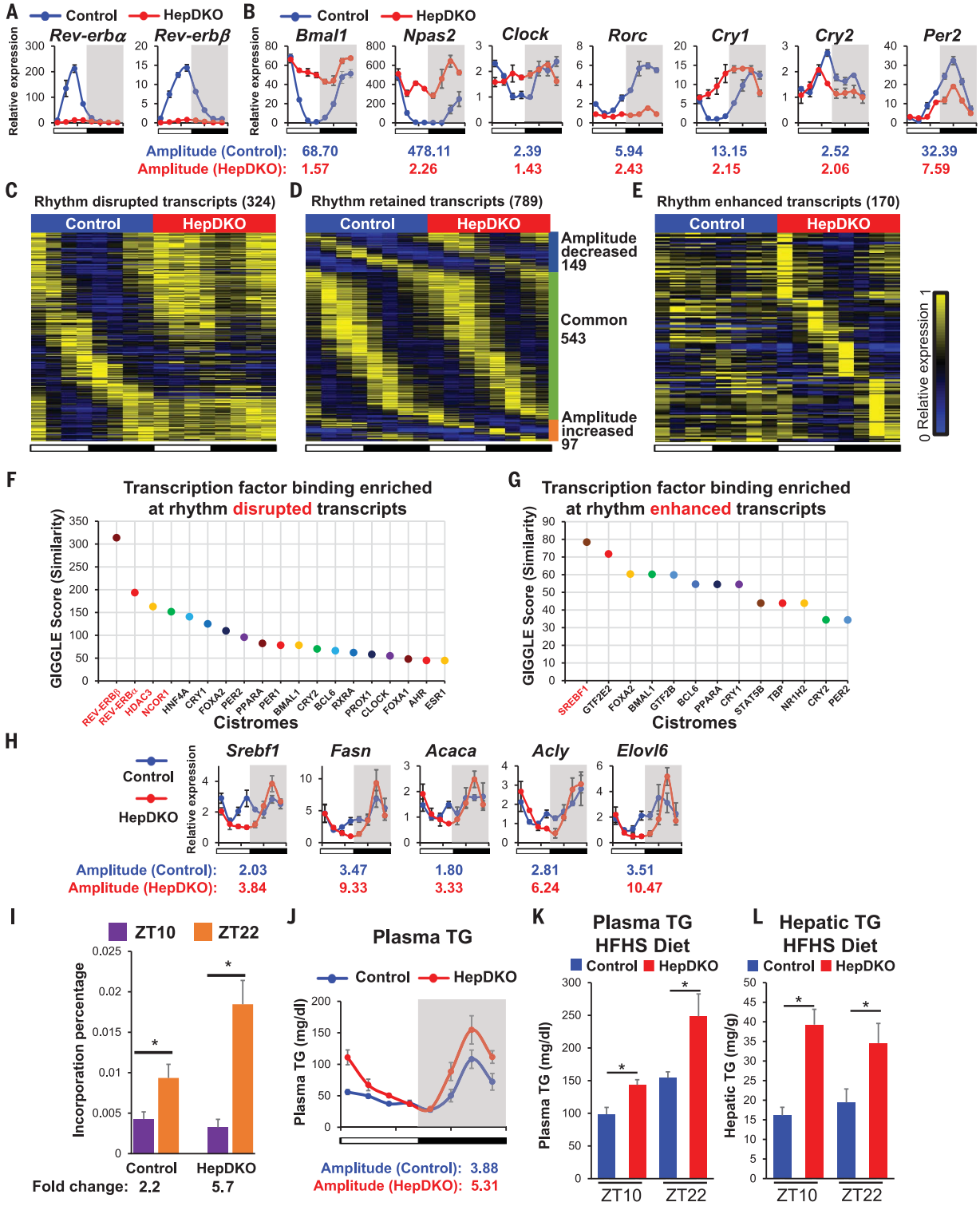

Fig. 1. Disruption of REV-ERBα and REV-ERBβ in hepatocytes remodels the liver diurnal rhythmic transcriptome and lipid metabolism. (**A** and **B**) Relative mRNA expression of *Rev-erbα* and *Rev-erbβ* (A) and REV-ERBs target genes (B) in control and HepDKO livers. (**C** to **E**) Heatmap of the relative expression of rhythm disrupted (C), retained (D), and enhanced (E) transcripts in control and HepDKO livers. The color bar indicates the scale used to show the expression of transcripts across eight time points, with the highest expression normalized to 1. JTK_CYCLE (*48*), adjusted $P < 0.01$, 21 hours ≤ period (t) ≤ 24 hours, peak-to-trough ratio > 2 (n = 3 mice per time point). (**F** and **G**) TF binding similarity screening on rhythm disrupted (F) and enhanced (G) transcripts based on all published liver cistromes from CistromeDB (*13*). (**H**) Relative mRNA expression of *Srebf1* and its target genes in control and HepDKO livers (n = 4 to 6 mice per time point). (**I**) Incorporation of deuterated water into liver fatty acids was measured in mice 6 hours after oral gavage of D_2O at ZT8 or ZT20. Data are presented as mean ± SEM. *$P < 0.05$ in Student's t test (n = 6 mice per group). (**J**) Serum triglyceride (TG) measurements in control and HepDKO mice. (**K** and **L**) Serum TG (K) and hepatic TG (L) measurements in HFHS-fed control and HepDKO mice. Data are presented as mean ± SEM (n = 4 to 6 mice per time point).

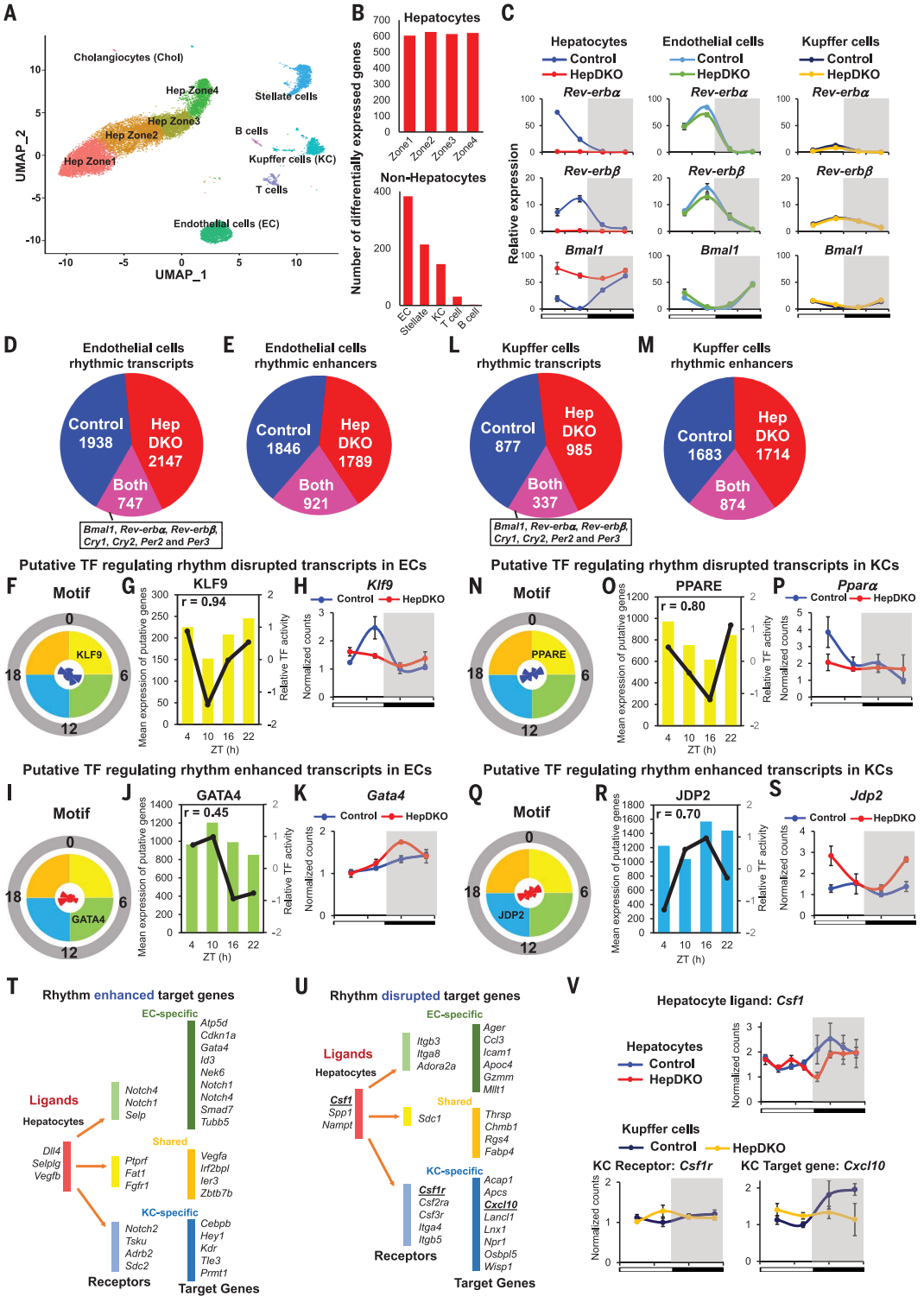

Fig. 2. Hepatocyte REV-ERBs control nonhepatocytic diurnal rhythmic transcriptomes. (**A**) Uniform manifold approximation and projection (UMAP) visualization of liver cell clusters based on 18,239 single-cell transcriptomes. (**B**) The number of differentially expressed transcripts in hepatocytes (top) or nonhepatocytes (bottom) upon REV-ERBs HepDKO. (**C**) Relative mRNA expression of *Rev-erbα*, *Rev-erbβ*, and *Bmal1* in isolated hepatocytes, ECs, and KCs from control and HepDKO livers. (**D** and **E**) Identification of diurnal rhythmic transcripts (D) and enhancers (E) in isolated ECs from control and HepDKO livers. JTK_CYCLE, adjusted $P \leq 0.05$, 21 hours ≤ period (t) ≤ 24 hours, peak-to-trough ratio > 1.5. (**F** and **I**) Rose diagrams showing the prevalence of rhythmic transcripts in each phase group, and motifs enriched at sites of rhythmic enhancers, which were correlated with rhythm disrupted (F) and enhanced (I) transcripts and enhancers from IMAGE in isolated ECs. (**G** and **J**) Correlation of mean expression of putative target genes and relative TF transcription activity in four phase groups in isolated ECs from control (G) and HepDKO (J) livers. In each plot, the bars represent the mean expression of putative TF target genes of each phase, and the black line represents the predicted TF relative transcription activity. Correlation coefficient r shows the strength of the relationship between the mean expression of putative TF target genes and relative transcription activity. (**H** and **K**) Expression level (normalized read counts) of *Klf9* (H) and *Gata4* (K) in isolated ECs from control and HepDKO livers. (**L** and **M**) Identification of diurnal rhythmic transcripts (L) and enhancers (M) in isolated KCs from control and HepDKO livers. (**N** and **Q**) Rose diagrams showing the prevalence of rhythmic transcript in each phase group, and motifs enriched at sites of rhythmic enhancers, which were correlated with rhythm disrupted (N) and enhanced (Q) transcripts and enhancers from IMAGE in isolated KCs. (**O** and **R**) Correlation of mean expression of putative target genes and relative TF transcription activity in four phase groups in isolated KCs from control (O) and HepDKO (R) livers. In each plot, the bars represent the mean expression of putative TF target genes of each phase, and the black line represents the predicted TF relative transcription activity. Correlation coefficient r shows the strength of the relationship between the mean expression of putative TF target genes and relative transcription activity. (**P** and **S**) Expression level (normalized read counts) of *Pparα* (P) and *Jbp2* (S) in isolated KCs from control and HepDKO livers. Data are presented as mean ± SEM (n = 4 mice per time point). (**T** and **U**) Ligand-receptor interaction analysis. Top three putative ligands from hepatocytes affect receptors (in ECs and KCs) for the regulation of rhythm enhanced (T) and disrupted (U) transcripts in ECs and KCs. (**V**) Examples of rhythm disrupted ligand (*Csf1*) from hepatocytes, receptor (*Csf1r*), and rhythm disrupted target gene (*Cxcl10*) in KCs.

are required to maintain lipid metabolism homeostasis.

Although hepatocytes are the most abundant cell type in the liver, the organ is composed of many other cell types that have critical roles in metabolic diseases (*17*–*19*). To better understand the effects of hepatocyte clock disruption, we performed single-nucleus RNA sequencing (sNuc-seq) on livers harvested at ZT8, when REV-ERBs are highly expressed, from control and HepDKO mice. sNuc-seq avoided skewing the results against lipid-laden hepatocytes that may be lost because of lysis or size exclusion during single-cell isolation, and ~3000 genes were detected per nucleus. On the basis of cell-specific markers (fig. S4, A and B), populations of hepatocytes, endothelial cells (ECs), Kupffer cells (KCs), stellate cells, and immune cells were clearly distinguishable, as were the subpopulations of hepatocytes corresponding to the previously defined markers of zonation (*20*) (Fig. 2A). As expected, many changes in gene expression were observed between control and HepDKO hepatocytes (Fig. 2B), with about two-thirds of the changes being common to hepatocytes in different zones (fig. S4C). The percentage of different cell populations in the liver was largely unchanged (fig. S4D), but gene expression in nonhepatocyte cells in the REV-ERB HepDKO livers was markedly altered, with the largest number of changes observed in ECs (Fig. 2B). Considerable changes were also noted in KCs, which are liver-resident macrophages that have critical roles within the organ (*17*). Together, these two cell types were selected for more detailed studies.

To quantify whole-cell transcriptomes with greater depth than is possible using sNuc-Seq, we performed diurnal rhythmic transcriptomics on ECs and KCs isolated every 6 hours, 2 weeks after hepatocyte-specific deletion of REV-ERBs. The deletion of *Rev-erbα* and *Rev-erbβ*, along with their constitutively induced repression target *Bmal1*, was confirmed in isolated hepatocytes. *Rev-erbα*/β gene expression was virtually unchanged in the ECs and KCs from the HepDKO livers, although the amplitude of *Rev-erbα*/β rhythms was muted in KCs (Fig. 2C). The relative expression of lineage-specific markers *Stab2* (ECs) and *Csf1r* (KCs) confirmed the specificity of the cell populations (fig. S4E).

Despite the physiologically rhythmic expression of the core clock genes, the diurnal rhythmic transcriptomes were extensively remodeled in ECs (Fig. 2D, fig. S5A, and table S3). These results indicated that disruption of the hepatocyte clock was communicated to the ECs. In addition, we quantified enhancer RNA expression in isolated ECs by mapping RNA-seq reads to intergenic regions of open chromatin determined by assay for transposase-accessible chromatin using sequencing (ATAC-seq) (*21*), which identified a widespread reprogramming of rhythmic enhancers (Fig. 2E, fig. S5B, and table S3).

We next used integrated analysis of motif activity and gene expression (IMAGE) (*22*) to ascertain sequence motifs enriched at sites of rhythmic enhancers associated with rhythmic genes to identify potential TFs with corresponding binding preferences and diurnal

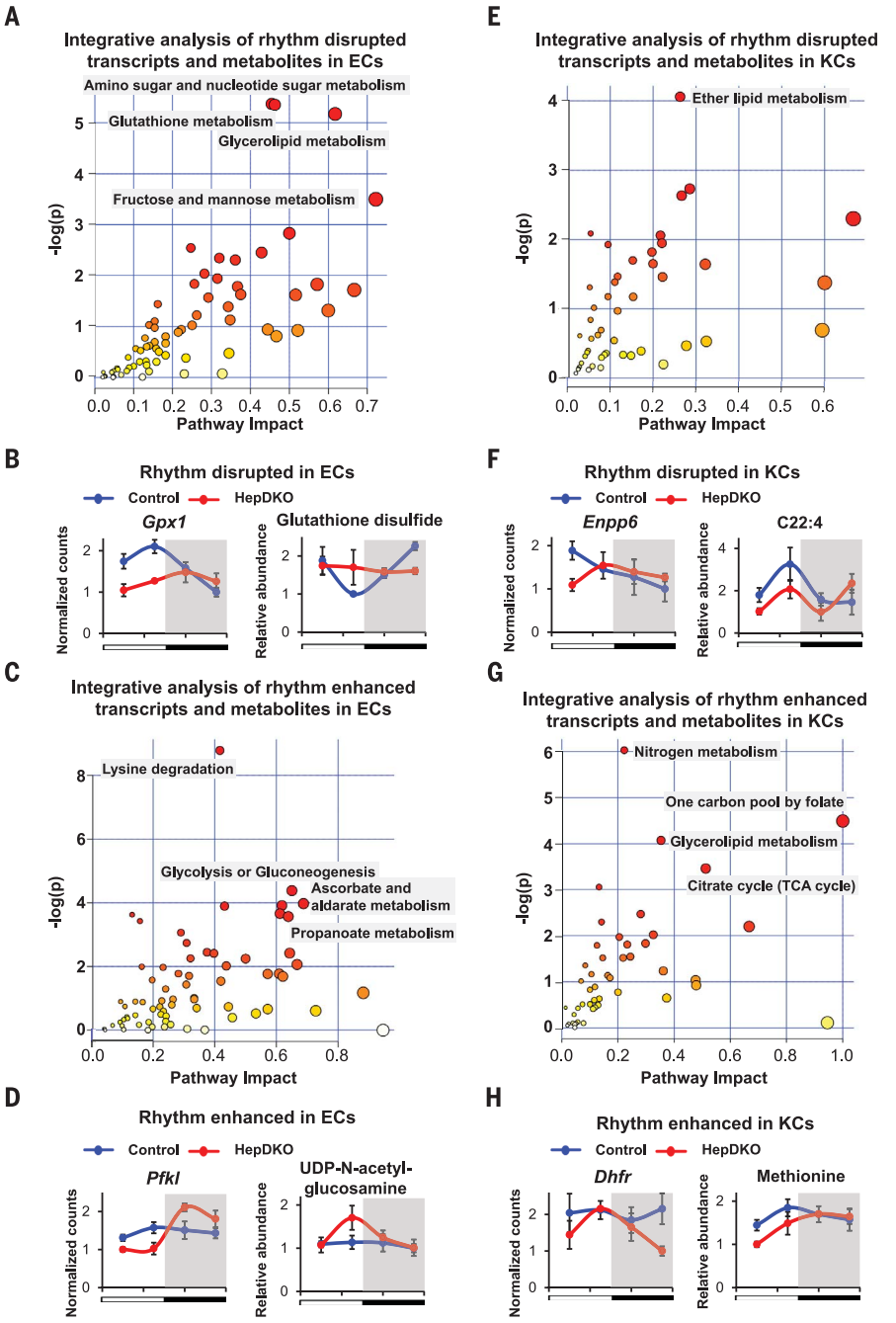

Fig. 3. Hepatocyte REV-ERBs regulate nonhepatocytic diurnal rhythmic metabolic process. (**A** and **C**) Metabolic pathway analysis integrating the enrichment of genes and metabolites in rhythm disrupted (A) and enhanced (C) transcripts and metabolites in isolated ECs. (**B** and **D**) Examples of rhythm disrupted (B) and enhanced (D) metabolites and related transcripts in ECs upon REV-ERBs DKO in hepatocytes. (**E** and **G**) Metabolic pathway analysis integrating the enrichment of genes and metabolites in rhythm disrupted (E) and enhanced (G) transcripts and metabolites in isolated KCs. (**F** and **H**) Examples of rhythm disrupted (F) and enhanced (H) metabolites and related transcripts in KCs upon REV-ERBs DKO in hepatocytes. Pathways were considered significant if $P < 0.01$ using hypergeometric test. Metabolites and transcripts data are presented as mean ± SEM (n = 3 or 4 mice per time point).

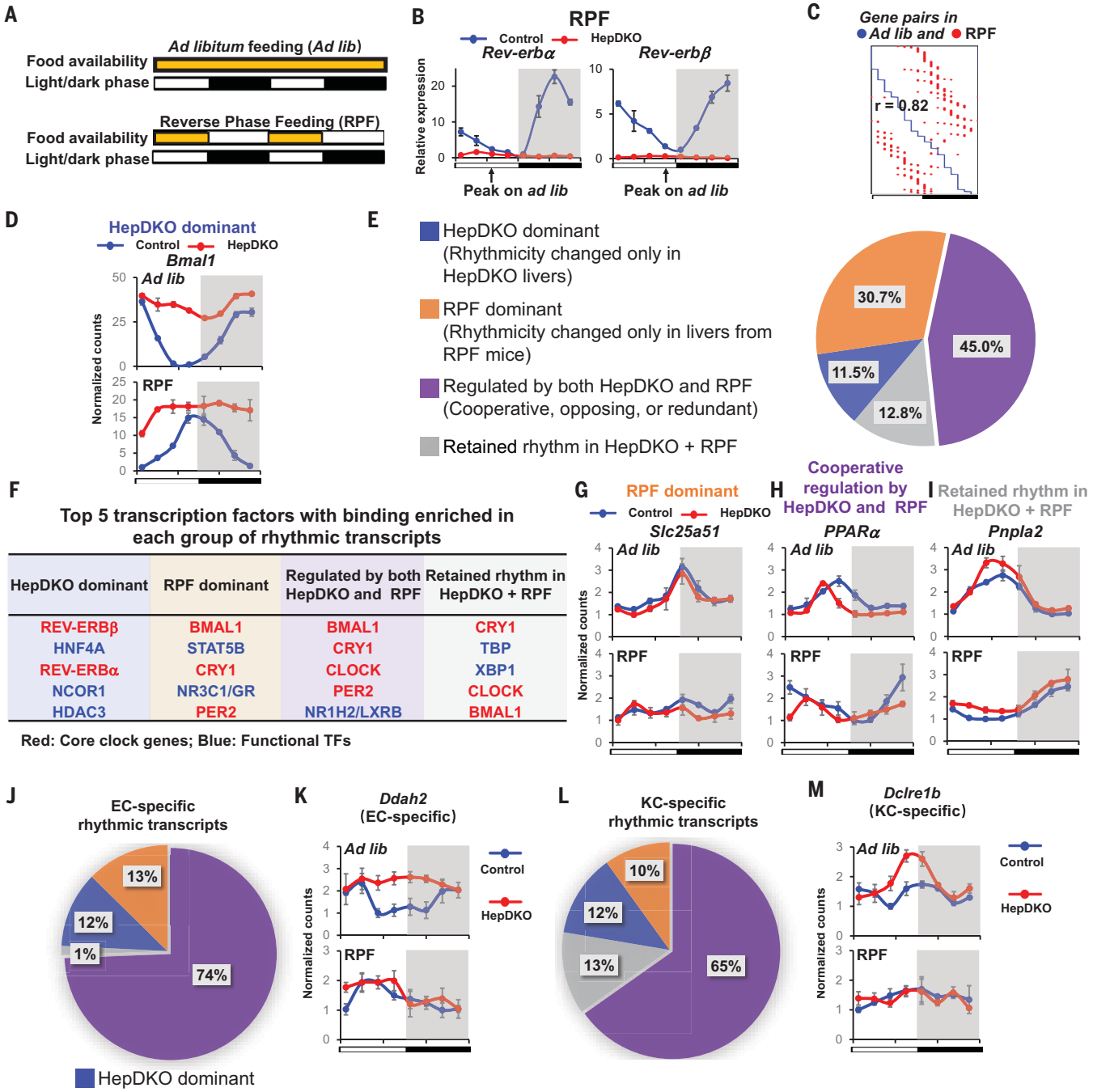

Fig. 4. Control of liver diurnal rhythms by the hepatocyte clock and feeding. (**A**) Diagram of feeding schedule of ad lib feeding and RPF. (**B**) Relative expression of *Rev-erbα* and *Rev-erbβ* in control and HepDKO livers from RPF mice. (**C**) Phase correlation of hepatic rhythmic transcripts between ad lib and RPF mice. Each row has a unique pair of hepatic rhythmic transcripts in ad lib mice (blue dot) and RPF mice (red dot). (**D**) Expression level (normalized read counts) of *Bmal1* in control and HepDKO livers from ad lib and RPF mice. (**E**) Identification of rhythmic transcripts that were dominantly regulated by HepDKO (blue) or RPF (orange), regulated by both HepDKO and RPF (purple), or retained in HepDKO+RPF (gray). (**F**) Top five TFs from four groups in (E) identified from TF binding similarity screening based on all published liver cistromes from CistromeDB (*13*). (**G** to **I**) Expression level (normalized read counts) of *Slc25a51*, *Pparα*, and *Pnpla2* in control and HepDKO livers from ad lib and RPF mice. (**J** and **L**) Identification of EC-specific (J) and KC-specific (L) rhythmic transcripts that were dominantly regulated by HepDKO (blue) or RPF (orange), regulated by both HepDKO and RPF (purple), or retained in HepDKO+RPF (gray). (**K** and **M**) Expression level (normalized read counts) of EC-specific gene *Ddah2* (K) and KC-specific gene *Dclre1b* (M) in control and HepDKO livers from ad lib and RPF mice. Data are presented as mean ± SEM (*n* = 3 mice per time point).

rhythmicity. These putative factors that were potentially responsible for rhythm disrupted and enhanced enhancers and transcripts were identified (table S4). For example, Kruppel-like factor 9 (KLF9), a ubiquitous regulator of oxidative stress (*23*), was identified as one of the putative TFs responsible for the loss of rhythmic enhancers associated with lost rhythmic genes that peaked between ZT0 and ZT6 (fig. S5C and Fig. 2F), and there was a positive correlation between KLF9 transcription activity and its putative target gene expression (Fig. 2G). Indeed, the expression of *Klf9* was rhythmic in control cells but not in ECs from HepDKO livers (Fig. 2H). Conversely, gained rhythmic enhancers peaking between ZT6 and ZT12 (fig. S5D and Fig. 2I) were enriched for the GATA-binding motif (Fig. 2J), corresponding to a gained rhythmic expression of *Gata4*, a known regulator of the hepatic microvasculature (*24*) (Fig. 2K).

Similarly, the KC rhythmic transcriptome was extensively reprogrammed in REV-ERB HepDKO livers (Fig. 2L, fig. S5E, and table S5), and this was associated with both the loss and gain of rhythmic enhancers (Fig. 2M, fig. S5F, and table S5). The factors identified as potentially responsible for rhythmic disrupted and enhanced enhancers and transcripts are listed in table S4. As an example, the PPAR-binding motif was enriched at sites of ZT0 to ZT6 rhythmic enhancers that decreased in KCs of the HepDKO livers (fig. S5G and Fig. 2N) and was associated with the highest transcriptional activity in this phase (Fig. 2O). Consistent with the transcriptional activity, the expression of *Pparα*, a regulator of the macrophage inflammatory response (*25*), was also rhythmic, peaking between ZT0 and ZT6 in control cells but not in KCs isolated from HepDKO livers (Fig. 2P). In contrast, the motif of Jun dimerization protein 2 (JDP2) was enriched in REV-ERB HepDKO-specific enhancers whose activity peaked between ZT12 and ZT18 (fig. S5H and Fig. 2Q) and also had the highest predicted transcriptional activity in this phase (Fig. 2R). The phase of the gained rhythmic expression of JDP2 was antiphase to its transcriptional activity (Fig. 2S), consistent with its transcriptional repression function (*26*). Moreover, comparative analysis of rhythmic remodeled transcripts between hepatocytes, ECs, and KCs revealed little overlap between different cell types, indicating a cell type–specific response to loss of REV-ERB in hepatocytes (fig. S6, A to C).

To uncover potential signals from hepatocytes lacking REV-ERBs to other cell types, we used NicheNet (*27*) to identify ligand-receptor pairs in which the ligand was altered in HepDKO hepatocytes, and the receptor was expressed in ECs, or KCs and the downstream genes exhibited enhanced (Fig. 2T and fig. S6D) or disrupted (Fig. 2U and fig. S6E) rhythms. For example, the colony stimulating factor 1 gene *Csf1* lost rhythmicity in HepDKO hepatocytes (Fig. 2V). The CSF1 receptor was expressed in KCs, and although it was not rhythmically expressed, downstream genes of the CSF1 signaling pathways such as *Cxcl10 (28)* lost rhythmicity (Fig. 2V). These results demonstrate how disruption of the hepatocyte clock could lead to altered diurnal rhythms of gene expression in surrounding nonhepatocytic cells. Note that this analysis does not incorporate posttranscriptional regulation of predicted ligands and receptors that were not regulated at the transcript level (table S6) (*29*).

To understand the impact of HepDKO-induced diurnal rhythm remodeling on nonhepatocytic cells, we performed GSEA on the rhythmic transcriptomes of ECs and KCs. Lipid metabolism–related pathways were found to be enriched in both ECs and KCs (fig. S7, A and B). This rhythm remodeling may be regulated not only via mapped ligand-receptor pairs but also via metabolites from hepatocytes, because we observed rhythmic metabolome reprogramming in isolated hepatocytes in the liver upon depletion of REV-ERBs (fig. S7, C and D, and table S7). Consistently, mouse phenotype enrichment analysis (*30*) indicates that phenotypes most enriched in altered rhythmic transcripts of both ECs and KCs from HepDKO livers were related to homeostasis and metabolism (fig. S7, E and F).

To test this prediction, we performed diurnal rhythmic metabolomic profiling, identifying many metabolites whose diurnal rhythms were disrupted or enhanced in ECs and KCs from HepDKO livers (fig. S7G and table S7). Integrated analysis of rhythm-remodeled transcripts and metabolites by MetaboAnalyst (*31*) revealed a number of significantly affected metabolic pathways. In ECs, multiple rhythmic metabolic pathways were disrupted, including glutathione metabolism (Fig. 3A and fig. S8), as illustrated by expression of the *Gpx1* gene and glutathione disulfide (Fig. 3B). Other pathways exhibited enhanced diurnal rhythmicity, including glucose metabolism and its conversion into hexosamines (Fig. 3C), as illustrated by the gained rhythm of *Pfkl* gene expression and uridine diphosphate-*N*-acetyl-glucosamine levels (Fig. 3D). These changes likely affect the function of ECs, which rely on glycolysis for energy production, with the hexosamine pathway controlling nitric oxide (NO) production and angiogenesis (*32*). In KCs, the correlated rhythmic disrupted transcripts and metabolites were related to lipid metabolism (Fig. 3E), exemplified by *Enpp6* gene expression and docosatetraenoic acid (C22:4) levels (Fig. 3F) (*33*, *34*), whereas rhythm enhanced pathways included one-carbon metabolism (Fig. 3G) regulated by the *Dhfr* gene (Fig. 3H). Together, the cell type–specific rhythm remodeling in nonhepatocytic cells upon the loss of hepatocyte REV-ERBs identifies a previously unknown, coordinated response to hepatocyte clock disturbance.

Although light-dark cycles act as zeitgebers to entrain behavioral rhythms via the central rhythmic oscillator in the SCN of the hypothalamus, feeding-fasting cycles are important synchronizers of peripheral clocks (*35*–*37*), and time-restricted feeding uncouples liver rhythms from behavioral rhythms (*35*). Having demonstrated the role of the hepatocyte clock in controlling cell-autonomous and non-cell-autonomous rhythms in the liver, we next considered its role in the response to nutrition by performing diurnal rhythmic transcriptomic analysis on mice subjected to 3 weeks of RPF, in which food was available only during the light phase (Fig. 4A). As expected, based on previous work (*35*), RPF of control mice led to a 12-hour phase shift in the rhythms of core clock genes such as *Rev-erbα* and *Rev-erbβ* (Fig. 4B). Transcriptomic analysis indicated that nearly all rhythmic transcripts exhibited a 12-hour phase shift in the livers of control mice under RPF (Fig. 4C), suggesting a dominant role of feeding on rhythmic phase regulation.

The rhythm of the core clock gene *Bmal1* was also phase shifted by ~12 hours under RPF in control livers. In contrast, in the livers of REV-ERB HepDKO mice, *Bmal1* expression was constitutive, robust, and nonrhythmic both under RPF and ad libitum (ad lib) feeding (Fig. 4D), indicating cell-autonomous clock regulation of the hepatocyte endogenous clock by REV-ERBs. Because most rhythmic genes were phase shifted ~12 hours by RPF, we assessed changes in rhythmicity using a classification that integrated amplitude (fold change of peak-to-trough ratio > 2), period (between 21 and 24 hours), and adjusted *P* value (<0.01) from the JKT algorithm (*38*). This analysis identified four categories of rhythmic genes: (i) HepDKO dominant (rhythmicity of transcripts is changed only in HepDKO livers); (ii) RPF dominant (rhythmicity of transcripts is changed only in livers from RPF mice); (iii) regulated by both HepDKO and RPF (including cooperative, redundant, or opposing changes); and (iv) retained rhythm in HepDKO and RPF (rhythmicity unchanged in HepDKO+RPF).

Of all rhythmic transcripts, 11.5% were HepDKO dominant (Fig. 4E, fig. S9A, and table S8A), and on the basis of TF binding similarity screening analysis, this group of rhythmic transcripts was likely directly regulated by REV-ERB and its corepressor complexes (Fig. 4F). RPF-dominant transcripts represented 30.7% of rhythmic transcripts (Fig. 4E and table S8B), implying non-cell-autonomous regulation by feeding. For example,

the diurnal rhythmicity of *Slc25a51* was indistinguishable in control and HepDKO livers from ad lib fed mice but disrupted in both control-RPF and HepDKO-RPF livers (Fig. 4G). Binding sites for STAT (signal transducer and activator of transcription) and GR (glucocorticoid receptor) TFs were enriched near these genes (Fig. 4F) (*39*, *40*).

Forty-five percent of rhythmic transcripts were regulated by both HepDKO and RPF, either cooperatively, oppositely, or redundantly (Fig. 4E and fig. S9B). Binding sites enriched near these genes included those of lipid-regulating liver X receptor (Fig. 4F), whose activation was reported to be rhythmically enhanced in livers of REV-ERBα whole-body knockout mice (*15*). Cooperative changes were exemplified by the *Pparα* gene (Fig. 4H and table S8C). Note that these results largely reflect hepatocytes, whose *Pparα* expression pattern was different from that shown for KCs. In contrast, the HepDKO-induced diurnal rhythmic enhancement of *Phf8* was negated by RPF while the rhythmic disrupting effect by RPF on *Ccnd1* was counteracted by HepDKO (fig. S9, B and C). The cooperative and opposing effects on rhythmicity demonstrate interdependence of the hepatocyte clock and feeding. However, for genes classified as redundant, the separate effects of HepDKO and RPF on rhythmicity were similar to each other and to the combination (e.g., *Srebf1*) (fig. S9, B and D).

In the final group of rhythmic transcripts, although the phase was dependent on food entrainment, the rhythmicity per se was retained in both HepDKO and RPF, suggesting that the rhythmic expression of transcripts in this group was controlled by other signals independent of the intrinsic clock and feeding (Fig. 4, E and I, and table S8D). Interestingly, although the rhythmic mRNA expression of core clock genes *Bmal1*, *Cry1*, and *Per2* was attenuated upon REV-ERB depletion, the binding sites were still enriched in these nonintrinsic rhythmic transcripts (Fig. 4F), suggesting that systemic signals drive the rhythmic transcription activity of these TFs (*14*, *41*).

Finally, we sought to determine the extent to which the hepatocyte clock and feeding-fasting cycles control diurnal rhythms in nonhepatocytes. We defined the EC-specific rhythmic genes using RNA-seq data from ECs isolated from the HepDKO livers and then determined their rhythmic expression during RPF, both in control and REV-ERB HepDKO livers. Notably, ~74% of rhythmic genes (Fig. 4J and Table S9A) were regulated by both HepDKO and RPF, with enrichment for genes regulating NO synthesis (fig. S9E), including EC-specific *Ddah2* (*42*) (Fig. 4K). Similarly, in KCs, ~65% of cell-specific rhythmic genes were regulated by both HepDKO and RPF (Fig. 4L and table S9B), with enrichment for genes regulating histone-serine phosphorylation (fig. S9F), including *Dclre1b*, which regulates DNA repair (*43*) and whose rhythmic expression was KC-specific in the liver (Fig. 4M). Thus, nonautonomous signals resulting from feeding and communication from hepatocytes play vital roles in the rhythmic gene expression of nonhepatocytic cells in the liver.

Our studies shed light on the physiological importance and function of peripheral clocks, whose existence was originally established in vitro (*44*–*46*). We demonstrate that some but not all hepatocyte diurnal rhythms are controlled by the core clock in a cell-autonomous manner in vivo. Moreover, the enhanced diurnal rhythms upon REV-ERB deletion (e.g., DNL genes) suggest that the clock not only anticipates daily environment changes but also buffers against certain fluctuations. Previous studies manipulating the liver clock found that it was not essential for weight loss due to food restriction during the normal feeding period (*47*) or behavioral diurnal rhythms for which the light-dark cycle acts as a zeitgeber (*7*). However, when feeding is restricted to the light phase, it becomes the predominant hepatocytic zeitgeber for the liver (*35*), and our studies demonstrate the hierarchy and interdependence of feeding and the cell-autonomous clock for diurnal rhythmic hepatocyte gene expression. Moreover, rhythmic gene expression and metabolism in nonhepatocytic cells in the liver are highly influenced both by the hepatocyte clock and feeding. These findings are likely to apply to peripheral clocks in other cell types.

REFERENCES AND NOTES

1. J. Bass, J. S. Takahashi, *Science* **330**, 1349–1354 (2010).
2. J. S. Takahashi, *Nat. Rev. Genet.* **18**, 164–179 (2017).
3. D. K. Welsh, J. S. Takahashi, S. A. Kay, *Annu. Rev. Physiol.* **72**, 551–577 (2010).
4. C. B. Green, J. S. Takahashi, J. Bass, *Cell* **134**, 728–742 (2008).
5. S. Panda, *Science* **354**, 1008–1015 (2016).
6. E. Trefts, M. Gannon, D. H. Wasserman, *Curr. Biol.* **27**, R1147–R1151 (2017).
7. K. B. Koronowski *et al.*, *Cell* **177**, 1448–1462.e14 (2019).
8. M. K. Bunger *et al.*, *Cell* **103**, 1009–1017 (2000).
9. C. Crumbley, Y. Wang, D. J. Kojetin, T. P. Burris, *J. Biol. Chem.* **285**, 35386–35392 (2010).
10. F. Guillaumond, H. Dardente, V. Giguère, N. Cermakian, *J. Biol. Rhythms* **20**, 391–403 (2005).
11. Y. Zhang *et al.*, *Science* **348**, 1488–1492 (2015).
12. H. Cho *et al.*, *Nature* **485**, 123–127 (2012).
13. R. Zheng *et al.*, *Nucleic Acids Res.* **47**, D729–D735 (2019).
14. B. Kornmann, O. Schaad, H. Bujard, J. S. Takahashi, U. Schibler, *PLOS Biol.* **5**, e34 (2007).
15. G. Le Martelot *et al.*, *PLOS Biol.* **7**, e1000181 (2009).
16. C. Vollmers *et al.*, *Proc. Natl. Acad. Sci. U.S.A.* **106**, 21453–21458 (2009).
17. O. Krenkel, F. Tacke, *Nat. Rev. Immunol.* **17**, 306–321 (2017).
18. M. Xu *et al.*, *Cell* **178**, 1478–1492.e20 (2019).
19. X. Xiong *et al.*, *Mol. Cell* **75**, 644–660.e5 (2019).
20. K. B. Halpern *et al.*, *Nature* **542**, 352–356 (2017).
21. Z. Zhang *et al.*, *Nat. Commun.* **10**, 4562 (2019).
22. J. G. S. Madsen *et al.*, *Genome Res.* **28**, 243–255 (2018).
23. S. N. Zucker *et al.*, *Mol. Cell* **53**, 916–928 (2014).
24. C. Géraud *et al.*, *J. Clin. Invest.* **127**, 1099–1114 (2017).
25. C. N. Brocker *et al.*, *Am. J. Physiol. Gastrointest. Liver Physiol.* **312**, G283–G299 (2017).
26. C. Jin *et al.*, *Mol. Cell. Biol.* **22**, 4815–4826 (2002).
27. J. Bonnardel *et al.*, *Immunity* **51**, 638–654.e9 (2019).
28. T. Barrett *et al.*, *Nucleic Acids Res.* **41**, D991–D995 (2013).
29. F. Atger *et al.*, *Proc. Natl. Acad. Sci. U.S.A.* **112**, E6579–E6588 (2015).
30. M. P. Weng, B. Y. Liao, *Bioinformatics* **33**, 3505–3507 (2017).
31. J. Chong, D. S. Wishart, J. Xia, *Curr. Protoc. Bioinformatics* **68**, e86 (2019).
32. P. Stapor, X. Wang, J. Goveia, S. Moens, P. Carmeliet, *J. Cell Sci.* **127**, 4331–4341 (2014).
33. G. D. Norata *et al.*, *Immunity* **43**, 421–434 (2015).
34. W. Wahli, L. Michalik, *Trends Endocrinol. Metab.* **23**, 351–363 (2012).
35. F. Damiola *et al.*, *Genes Dev.* **14**, 2950–2961 (2000).
36. B. J. Greenwell *et al.*, *Cell Rep.* **27**, 649–657.e5 (2019).
37. F. Mange *et al.*, *Genome Res.* **27**, 973–984 (2017).
38. M. E. Hughes *et al.*, *J. Biol. Rhythms* **32**, 380–393 (2017).
39. A. Kalvisa *et al.*, *PLOS Biol.* **16**, e2006249 (2018).
40. F. Quagliarini *et al.*, *Mol. Cell* **76**, 531–545.e5 (2019).
41. E. L. McDearmon *et al.*, *Science* **314**, 1304–1308 (2006).
42. A. J. Pope, K. Karrupiah, P. N. Kearns, Y. Xia, A. J. Cardounel, *J. Biol. Chem.* **284**, 35338–35347 (2009).
43. J. Ye *et al.*, *Cell* **142**, 230–242 (2010).
44. E. Nagoshi *et al.*, *Cell* **119**, 693–705 (2004).
45. R. Öllinger *et al.*, *J. Cell Sci.* **127**, 4322–4328 (2014).
46. J. C. Dunlap, *Cell* **96**, 271–290 (1999).
47. A. Chaix, T. Lin, H. D. Le, M. W. Chang, S. Panda, *Cell Metab.* **29**, 303–319.e4 (2019).
48. M. E. Hughes, J. B. Hogenesch, K. Kornacker, *J. Biol. Rhythms* **25**, 372–380 (2010).

ACKNOWLEDGMENTS

We thank H. J. Richter, K. Zhu, Y. Zhang, Y. H. Kim, and other members of the Lazar lab for technical support and valuable discussions, particularly during the revision of this manuscript while sheltered in place during the coronavirus pandemic. We thank J. G. S. Madsen and S. Mandrup for advice on using the IMAGE program. **Funding:** We thank the Functional Genomics Core and the Viral Vector Core of the Penn Diabetes Research Center (P30 DK19525) for next-generation sequencing and virus preparation, respectively. We also acknowledge the Penn DRC Metabolomics Core at Princeton (DK19525). This work was supported by the JPB Foundation (M.A.L.) and the Cox Medical Research Institute (M.A.L.), as well as by National Institutes of Health grants R01-DK045586 (M.A.L.) and F32DK116519 (D.G.). C.Ja. and W.H. were supported by American Diabetes Association Training Grants [1-17-PDF-076 (C.Ja.) and 1-18-PDF-132 (W.H.)]. P.D. was supported by a postdoctoral fellowship from the American Heart Association (20POST35210738). **Author contributions:** D.G. and M.A.L. conceptualized the study, interpreted data, and wrote the manuscript, which was revised and approved by all authors. D.G. performed RNA-seq, ATAC-seq, and bioinformatics analysis. Y.Xio. and T.M.T. performed real-time qPCR. D.G. and Y.Xia. performed sNuc-seq. C.Ji. performed IMAGE analysis. C.Ja. and J.D.R. designed and performed metabolomics and FA synthesis rate. Y.Xio., T.M.T., W.H., P.D., and D.G. assisted with animal husbandry. **Competing interests:** J.D.R. is a consultant for Pfizer, scientific adviser to Colorado Research Partners, and cofounder of Toran. M.A.L. is a consultant to Pfizer, Novartis, Madrigal Pharmaceuticals, and Calico. **Data and materials availability:** The GEO accession number for the RNA-seq, ATAC-seq, and sNuc-seq data reported in this paper is GSE143528. M.A.L. obtained REV-ERBβ floxed mice under a material transfer agreement with the Centre Europeen de Recherche en Biologie et Medecine.

SUPPLEMENTARY MATERIALS

science.sciencemag.org/content/369/6509/1388/suppl/DC1
Materials and Methods
Figs. S1 to S10
Tables S1 to S10
References (*49*–*60*)
MDAR Reproducibility Checklist

View/request a protocol for this paper from *Bio-protocol*.

14 January 2020; accepted 16 July 2020
10.1126/science.aba8984

Science

The hepatocyte clock and feeding control chronophysiology of multiple liver cell types

Dongyin GuanYing XiongTrang Minh TrinhYang XiaoWenxiang HuChunjie JiangPieterjan DierickxCholsoon JangJoshua D. RabinowitzMitchell A. Lazar

Science, 369 (6509),

Keeping rhythm requires communication

In mammals, daily cycles in physiology require the synchronized activity of circadian clocks in peripheral organs such as the liver, a hub of metabolism. Guan *et al.* generated mice with hepatocytes that lack two transcriptional repressors known to be essential for clock function. This experimental manipulation unexpectedly disrupted rhythmic gene expression and metabolism not only in hepatocytes but also in other liver cell types. Feeding behavior also coregulated circadian rhythms in multiple liver cell types. Cell-cell communication thus appears to be important in maintaining the robustness of peripheral circadian clocks.

Science, this issue p. 1388

Science (ISSN 1095-9203) is published by the American Association for the Advancement of Science. 1200 New York Avenue NW, Washington, DC 20005. The title *Science* is a registered trademark of AAAS.